Journal of Cleaner Production 292 (2021) 126018

Contents lists available at ScienceDirect

Journal of Cleaner Production

journal homepage: www.elsevier.com/locate/jclepro

Study on productivity and aerosol emissions of magnetic field-assisted EDM process of SiC_p/Al composite with high volume fractions

Zhen Zhang [a, b], Yi Zhang [a], Liquan Lin [a], Jinhong Wu [a], Haishen Yu [a], Xin Pan [a], Guangliang Li [a], Jie Wu [a], Tao Xue [a, *]

[a] School of Aerospace Engineering, Huazhong University of Science and Technology, Wuhan, Hubei, 430074, China
[b] Guangdong HUST Industrial Technology Research Institute, Guangdong Provincial Key Laboratory of Digital Manufacturing Equipment, Dongguan, 523808, China

ARTICLE INFO

Article history:
Received 27 February 2020
Received in revised form
10 January 2021
Accepted 15 January 2021
Available online 21 January 2021

Handling Editor: Cecilia Maria Villas Bôas de Almeida

Keywords:
EDM
SiCp/Al Composite
Aerosol emissions
Material removal rate
Electrode wear rate
Magnetic field

ABSTRACT

SiC particulate reinforced Al-based metal matrix composites with high volume fractions (HVF – SiC_p/Al) is widely applied in many engineering fields due to combining outstanding properties of both metal and ceramic materials. It's a tough problem to process HVF – SiC_p/Al with superior machining performance and minor environmental effect. Thus, in this paper, magnetic field assisted electrical discharge machining (MF-EDM) of HVF – SiC_p/Al is proposed to improve the sustainable machining performance including productivity and aerosol emissions which is most harmful to operators' health. Based on Taguchi method, a set of experiments are settled to investigate materials removal rate (MRR), electrode wear rate (EWR), and aerosol emissions under MF-EDM process of 45% and 65% SiC_p/Al. It shows that pulse current is the major factor, and magnetic field assisted technology significantly develops the surface integrity whereas it just slightly contributes to improve MRR, EWR, and aerosol emissions when the intensity of magnetic is in the range of 0.1T–0.2T. Additionally, an optimization algorithm combing Quantum-behaved Particle Swarm Optimization with Gaussian distributed local attractor (GAQPSO) and Back Propagation Neural Network (BPNN) is employed to provide optimal machining parameters for economic and environmental MF-EDM process of HVF – SiC_p/Al. Compared to the average experimental data, for 45% SiC_p/Al, the average optimal solutions of EWR, and aerosol emissions were decreased by about 10% and 15% whereas MRR was increased by about 6.6%; for 65% SiC_p/Al, the average optimal solutions of EWR, and aerosol emissions were decreased by about 5.7% and 10% whereas MRR was increased about by 5.5%. It presents an effective work for EDM process of HVF – SiC_p/Al with high sustainable performance.

1. Introduction

SiC particulate reinforced Al-based metal matrix composites (SiC_p/Al) have been considered as excellent candidates to be widely used as structural material in military services, aero engineering, automobile industry, and other areas due to combining outstanding properties of both metal and ceramic materials, such as high strength, high hardness and superior wear resistance (Xiong et al., 2011). However, the ceramic reinforced components (SiC_p) in the Al-based material results inefficient process, expensive cost and low process performance, especially for machining high volume fraction SiC_p/Al composites (HVF – SiC_p/Al) (Du et al., 2019; Gururaja et al., 2013). When cutting, milling or grinding of SiC_p/Al composites, material removal rate (MRR), tool wear rate (EWR, closed to tool life), and surface integrity are commonly considered as important indicators of machining performance and completely discussed by lots of researchers (Gururaja et al., 2013). For example, Bhushan (2013) investigated the influence of process parameters on CNC turning cutting output of 15% SiC/Al and multi-response optimized to obtain minimum the power consumption and maximum tool life via desirability analysis route. Recently, electrical discharge machining (EDM), which could directly melt and vaporize the workpiece via generating pulse discharge channel of more than 10k degree, was successfully implemented to machining of particle reinforced metal matrix composites (MMCs) due to its ability of no-contact machining of the difficult to process materials

* Corresponding author.
E-mail address: xuetao@hust.edu.cn (T. Xue).

https://doi.org/10.1016/j.jclepro.2021.126018
0959-6526/

Nomenclature

SiC_p/Al	Particulate reinforced Al-based metal matrix composites
HVF − SiC_p/Al	High volume fractions SiC_p/Al
EDM	Electrical discharge machining
MF	Magnetic field
MF-EDM	Magnetic field assisted EDM
MRR	Materials removal rate
EWR	Electrode wear rate
CA	Concentration of aerosols
GAQPSO	Quantum-behaved particle swarm optimization with Gaussian distributed local attractor
BPNN	Back propagation neural network
B	Magnetic field intensity
I	Pulse current
T_on	Pulse on time
T_off	Pulse off time
C_A	Concentration of aerosols
W_a	Weight of filter paper before sampling
W_b	Weight of filter paper after sampling
v	Sampling speed
t_s	Sampling duration
X_i	Position of the particle
U_i	Original local state of the particle
U_i'	New local state of the particle with Gaussian distribution N
Pb_i	Personal best state of the particle
Gb	Global best state of all the particles
m_i	The average of all the personal best states

with complex shapes (Pramanik, 2014; Kandpal et al., 2015). Based on the experimental research, Ming et al. (2016) established a soft computing model and intelligent optimization system with graphical user interface (GUI) to multi-objective optimize the EDM process of SiC_p/Al composites with desired MRR and surface roughness. While Tang et al. (2018) proposed a dynamic simulation tool to estimate the temperature field of EDM process of SiC/Al composites considering continuous discharge with multiple pulses, and studied the effect of peak current and pulse-on time on discharge pits and MRR. Although EDM process does well in machining of SiC_p/Al composites, the sustainability and environmental friendliness of EDM process of SiC_p/Al composites should be paid more attentions due to material removal mechanism based on the violent thermal effect of EDM process.

According to a study from United States Department of Commerce (USITC, 2009), a manufacture process can be called sustainable if it has the least negative environment influence, minimal consumption of energy and natural resources, and harmless to employees, communities, and consumers. Even though EDM is one of most important non-traditional machining techniques which accounts up over seven percent in the whole manufacture process market (Zhang et al., 2018). The EDM process is also unquestionable one of the least sustainable manufacturing machining method, the reason is that it consumes large energy, wears electrode frequently and releases harmful emissions but provides low productivity (Valaki et al., 2014). Thus lots of researchers focused on the improvement of sustainable performance in the EDM process, especially on the decreasing energy cost, electrode wear, and environment influence as well as increase of productivity (MRR). Maher et al. (2015) integrated an adaptive neuro-fuzzy inference system with Taguchi analysis strategy to improve the work rate and high grade of machined surface with fewer heat-affected area at possible minimum cost for sustainable wire EDM (WEDM) production. Considering environmental and manufacturing aspects, Garg and Lam (2016) completely analyzed the effects of energy consumption, dielectric consumption, and tool wear ratio (similar to EWR) on machining input of EDM, used genetic programming (GP) optimization algorithm to make the machining efficiency and environment conservative Gamage et al. (2016) not only assessed the environmental impact in the EDM process of aluminium (3003) and steel using life cycle analysis, but also worked on finding out the main parameters to optimize the process energy consumption and surface quality of WEDM of Inconel718 and Ti6Al4V so as to indirectly reduce carbon emissions (Gamage et al., 2017).

Additionally, the EDM process is still considered as hazardous to the operators as well as to the environment because pulse discharging between cathode and anode may release volumes of hazardous emissions containing toxic aerosols, gases, debris and sound pollution (Mathew et al., 2010a). Harmful releases generated by the EDM process is mainly relied on material removal mechanism, dielectric fluid, tool makings and workpiece makings (Sivapirakasam et al., 2011). In order to reduce the release of toxic emission products from EDM dielectrics, Valaki and Rathod (2015) evaluated and adopted refuse vegetable oil, which is a kind of biofluid, as a substituted dielectric fluid (like hydrocarbon oil and kerosene) to develop the sustainable performance with environmental friendliness, while Kou and Han (2018) proposed a sustainable EDM milling process with water-based dielectric, to increase productivity (MRR) and decrease the contamination to the environment. It's urgent to find out an appropriate method to improve sustainable machining performance of EDM for advanced materials, including MRR, EWR, and environmental impact.

Recently, some researchers demonstrated that magnetic field (MF) assisted EDM (MF-EDM) process could contribute to improve the machining performance with better surface quality and high productivity (Bains et al., 2018a, b). Heinz et al. (2011); Zhang et al. (2016); Chen et al. (2017) presented the material removal mechanism and discharged debris motion under the effect of external MF in the Micro-EDM and WEDM process.

Zhang et al. (2018) proposed the sustainable MF-EDM process for less energy cost and environmental harmfulness, and made optimization among the values of EWR, energy cost and process sound waste of MF-EDM. Moreover, Ming et al. (2019) conducted a comparative investigation on the efficient using of energy and influence of environment in MF-EDM as well as common EDM by use of combining simulation and experimental analysis. Zhang et al. (2020a) successfully implemented external MF assisted WEDM to improve the process accuracy and MRR as well as reduce energy consumption.

All these work reveal that using external MF has notably improved sustainable process capability on EDM, Mirco-EDM and WEDM. Thus, magnetic field assisted EDM technique is perhaps a good solution to machine SiC_p/Al composite, but few literatures focused on investigating sustainable machining performance of MF-EDM process of SiC_p/Al composite. In order to achieve high sustainability and environmental friendliness of ED machining SiC_p/Al composites, the material removal mechanism and environmental impact of MF-ED machining SiC_p/Al composites should be figured out before magnetic field assisted technique can be widely applied. Particularly, in this paper, a complete study on productivity and emissions of MF-EDM process of SiC_p/Al composites was carried out based on Taguchi method, aiming to

investigate the procedure of sustainable machining process. More over, to achieve better sustainable performance of MF-EDM process of HVF – SiC_p/Al, a multi-objective optimization algorithm combining Back Propagation Neural Network with Quantum-behaved Particle Swarm Optimization with Gaussian distributed local attractor (BPNN-GAQPSO) is presented. The function-in of the algorithm is a result set of experiment and the function-out is a set of Pareto optimal data. It uses a Gaussian distribution factor which can keep the diversity of the data hence provide better result than the algorithm by (Zhang et al., 2020b).

This work consists of five sections. Research background and introduction are made in the first section. Section 2 presents the principles of material removal mechanism and emissions of MF-EDM process of HVF – SiC_p/Al composites as well as the experiments for investigating MRR, EWR and aerosol emissions. In section 3, it analyzed the influence of main process parameters on MRR, EWR as well as aerosol emissions. The multi-objective optimization algorithm BPNN-GAQPSO is presented to optimize the MF-EDM process of HVF – SiC_p/Al composites in section 4. The research conclusion is given in the last section.

2. Experimental procedure

2.1. Mechanism of MF-ED machining SiC_p/Al composites

Since a high-temperature plasma channel is generated to melt and evaporate the material by pulse high-frequency voltage, EDM involves the formation of plasma channels and the removal of charged debris. The assisted magnetic field can change the free motion of the particles in the plasma channel into regular motion, which restricts the plasma expansion and contributes to efficiently remove charged debris.

Firstly, the external magnetic field could not only confine the radius of plasma channel based on the Larmor Radius Principle as well as increase the energy intensity of the plasma by creating smaller discharge spots and more electron collisions, but also improve the stability of plasma channel in EDM process. At the same time, the external magnetic field could also significantly affect the locations and distributions of spark discharge spots during MF-EDM process. Thus MF-EDM process contributed to improve machining performance with high MRR and low surface roughness, leading to a decrease in radius of discharge craters and an increase in depth and volume of discharge craters on workpiece surface. Thus the energy utilization efficiency and material removal rate of MF-EDM process is much better than that of the EDM, which directly reduce energy consumption and indirectly carbon emissions. Additionally, assisted magnetic field would affect the motion of charged particles via generating Lorentz force and help the debris be taken away from the discharge gap. The deposition of debris could be reduced during the MF-EDM process. No matter for magnetic or non-magnetic materials, the removed debris will be electrically charged by the pulsed discharge process of EDM when the debris leaving the machine surface of workpeice. Since the debris of non-magnetic materials will also take charged during the EDM process, and the magnetic field could still affect the motion of charged debris and contribute to a high efficiency of flushing debris. Specifically, the motion of charged particles existed in the discharge channel between cathode and anode are mainly affected by external magnetic field and self-excited electromagnetic field from changing electric field of the EDM process. But the excited electromagnetic field can be neglected because the external magnetic field is far larger than it when influencing the motion trajectory of charged particles. The detailed motion trajectory of charged particles was described as follows.

Under the effect of Lorentz force, the debris could be effectively taken away from the discharge gap of the EDM process, and then two representative actions of charged debris (external debris1 and internal debris2) are explained in Fig. 1.

At the beginning of MF-EDM process of SiC_p/Al composites, the external charged debris1 is produced between the bottom of electrode and top of workpiece, and subjected to Lorentz force $F_{v_{1y}}$ in Y direction (current is in Z direction and magnetic field is in X direction). On the surface of workpiece, the charged debris can be easily cleared with the velocity of V_{1y}, which prevents short circuit, multi-discharge or arc-discharge in order to develop the pulse discharge quality and machining performance.

Considering the internal charged debris 2 generated between the periphery of electrode and inside of material, the velocity V_{2x} in $X+$ direction is parallel to the direction of assisted MF, while the velocities of V_{2y} in $Y+$ direction and V_{2z} in $Z-$ direction are perpendicular to the direction of assisted MF. Thus $F_{v_{2y}}$ and $F_{v_{2z}}$ can be generated respectively in $Z+$ and $Y+$ direction except $X+$ direction by Lorentz force Equation ($F = qvB$). The resultant force of charged debris 2 leads to the debris moving away from the discharge gap.

The above analysis of two representative debris action and force reveals that Lorentz force in MF-EDM process can promote the debris effectively being flushing away the discharge gap, maintain the stability of discharge so that the process performance can be improved.

However, the ceramic reinforced components (SiC_p) in the Al-based material result in blocking the generation of normal discharge and debris motion between workpiece and tool electrode due to its feature of low conductivity. So the higher volume of SiC particles fraction in SiC_p/Al, the harder to machine by use of EDM. This is main reason for that is difficult process HVF – SiC_p/Al composites.

2.2. Materials

HVF – SiC_p/Al composites, namely 45% and 65% SiC volume fraction of SiC_p/Al composites (SiC particles take up 45% and 65% of the whole composite), which were fabricated by Xi' an MingKe Microelectronics Co. Ltd., are selected as the experimental materials. The shape of experimental material specimen is rectangular parallelepiped plate with the size of 40 × 150 × 40mm. The electrode used during machining is a copper cylinder with a diameter of 10 mm and a length of 80 mm. Additionally, Table 1 shows the main machining conditions of magnetic field assisted EDM process of 45% and 65% SiC_p/Al composites.

2.3. Aerosol emissions

Electrical discharge machining could directly melt and vaporize the workpiece HVF – SiC_p/Al composites via generating pulse discharge channel of more than 10k degree. During this violent thermo-physical process, at the spark location, some material of tool and workpiece will be dissolved, precipitated and/or condensed into the dielectric, whereas other exhaust will be released as gases and aerosols into aerosphere. The aerosols generated from this procedure may contain metal/metalloid particles (such as Al, Cu, Si, etc.), carbon powder and reaction products of dielectric fluid, which are easy and dangerous to be breathed by operators. Thus aerosol emissions from EDM process of HVF – SiC_p/Al is very harmful to the long time operators as well as to the work environment. More volume fraction particles of SiC leads more hazardous emissions generated in EDM process of HVF – SiC_p/Al. Fig. 2 shows massive emissions of fumes containing aerosols and gases from EDM process of HVF – SiC_p/Al.

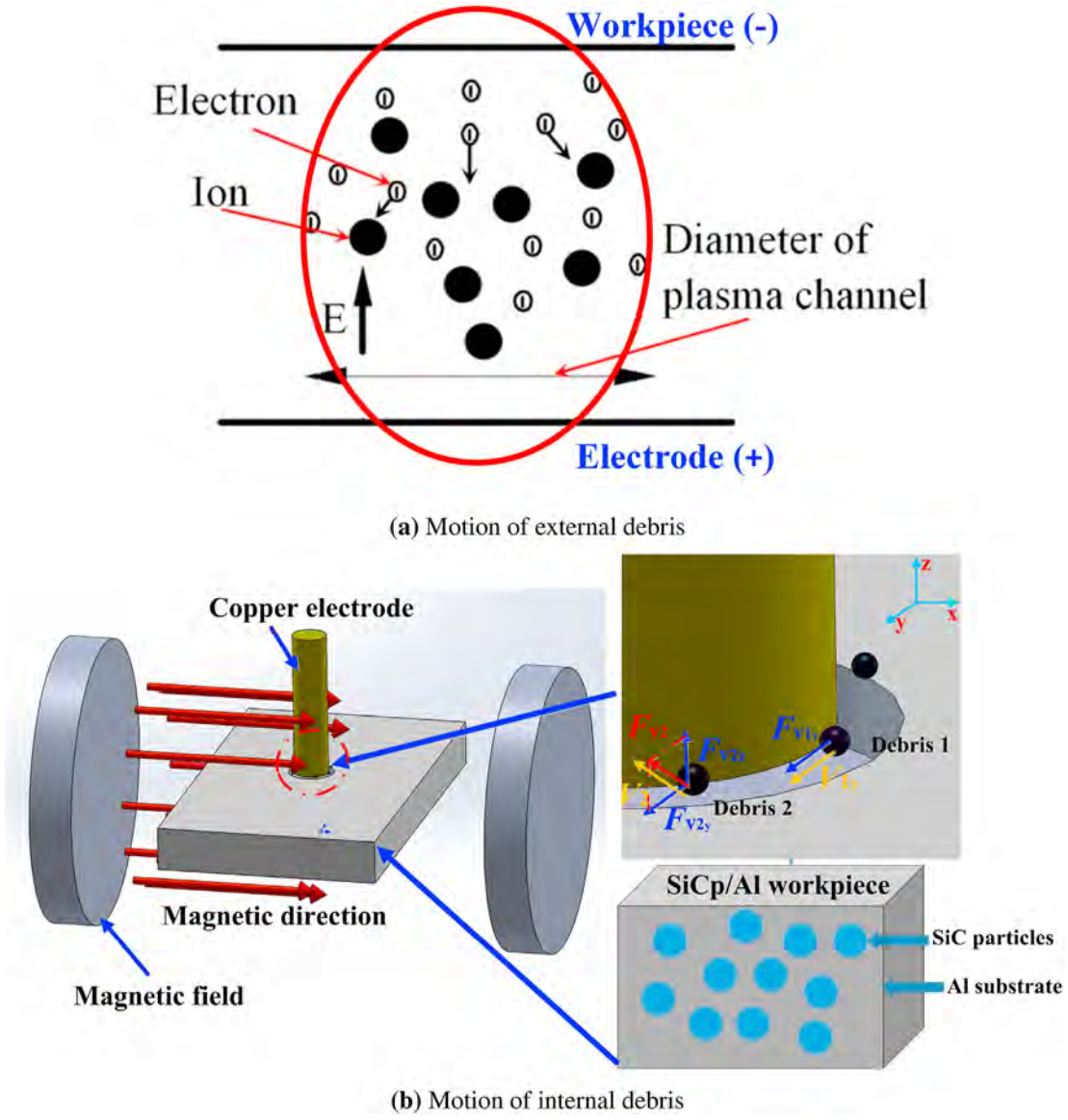

Fig. 1. Motion and force of charged debris in magnetic field assisted EDM process.

Table 1
Machining conditions of magnetic field assisted EDM.

Conditions	Values
Purity:SiC volume fractions (%)	45, 65
Workpiece Size (mm^3)	Rectangle, 40 × 150 × 4
Electrode Size (mm^3)	Cylinder, Diameter: 10, Length: 80
Feeding Direction	Vertical
Temperature (°C)	20
Dielectric	Kerosene oil
Electrode material	Copper

2.4. Experimental design

In this MF-EDM experiment, there are many factors influencing the sustainable machining performance, namely MRR, EWR, and aerosol emissions. After conducting preliminary exploratory experiments and lots of literature reviews, the main factors affecting the experimental results are pulse current (A), pulse-on time (T_on), pulse-off time (T_off), and magnetic field intensity (B), and each factor are set into four levels, which ranges in a sensible area for input variables based on the MF-EDM process of HVF − SiC_p/Al. According to the two different volume fraction of SiC_p/Al composites, two L16 orthogonal experiments with different parameter level are designed by use of Taguchi design method, as shown in Table 2.

2.5. Measurement

Main instrumentations includes the EDM equipment (GF Form350), the magnetic field setup (home-made), electronic balance (BSM220.4), Universal Air Sample with cyclone (SKC R8), thermal field emission scanning electron microscope (JSM-7600F), and high field depth digital microscope (Leica DVM6).

2.5.1. Material removal Rate(MRR)

As for each experimental set, the machining depth was set as 1.5 mm, while the same cylindrical electrode with a diameter of 10 mm was used in the MF-EDM process. The machining time was counted by a Stopwatch. So the MRR could be calculated by the

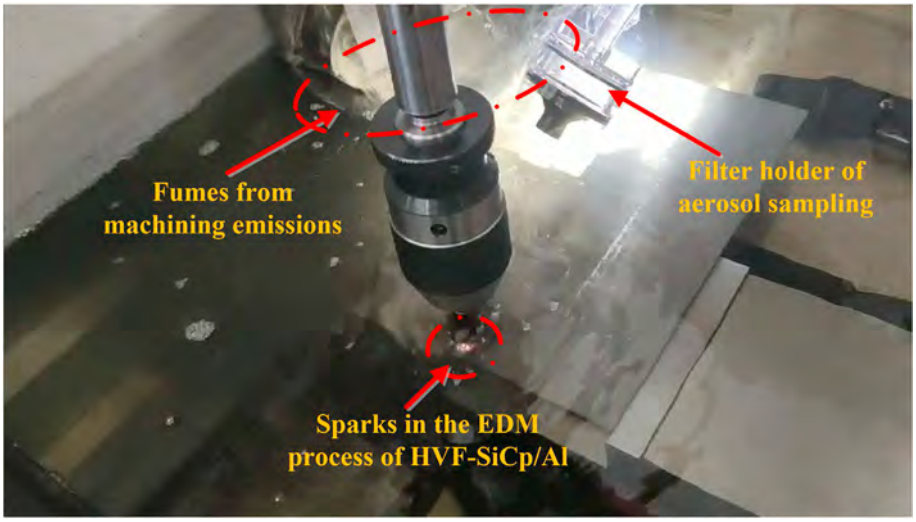

Fig. 2. Emission of fumes from the EDM process.

Table 2
Main Factors and their level for machining experiments (4 inputs and 4 levels).

Volume fraction of SiC_p/ Al	Parameters	I (A)	T_on (μs)	T_off (μs)	B (T)
	Symbol	I	T_on	T_off	B
45%	Levels	10	150	120	0
		15	180	140	0.1
		20	210	160	0.2
		25	240	180	0.3
65%	Levels	15	120	80	0
		20	150	100	0.1
		25	180	120	0.2
		30	210	140	0.3

following equation (1) (Chattopadhyay et al., 2008).

$$MRR = \frac{\pi \times 10^2 \times 1.5}{t} \quad (1)$$

where t is machining time (min), and the unit of MRR is (mm^3/ min).

2.5.2. Electrode wear rate (EWR)

The electrode wear is accompanied with the material removal process by pulse discharge spark, and EWR is the weight loss of electrode per unit time, an indicator to express the amount of electrode wear during the EDM process. It is very important to machining accuracy and exhaust emissions of EDM process.

As for two L16 experimental groups, a total of 32 non difference copper cylindrical electrodes were used in each experiment set. By use of an electronic balance (BSM220.4) with a resolution of 0.001g, the weight of electrodes (m_1) were measured before the ED machining experiments. Then the debris attached to electrodes would be washed away by ultrasonic cleaner to achieve more accurate weight of electrodes. The weight of electrodes (m_2) were measured after the ED machining and ultrasonic cleaning by use of the same electronic balance. So the weight loss of electrode can be obtained by $m_1 - m_2$. All the measurement values were conducted for three times to obtain their mean values. The machining time (t) was counted by a Stopwatch. Finally the EWR could be calculated by the following equation (2) (Chattopadhyay et al., 2008).

$$EWR = \frac{m_1 - m_2}{t} \quad (2)$$

where, m_1 is Mass of electrode before EDM process (mg), m_2 is mass of electrode after EDM process (mg), t is the machining time (min), and the unit of EWR is (mg/min).

2.5.3. Aerosol emission collection method

In order to accurately evaluate the aerosol emission during the EDM process, an experimental setup for aerosol sampling in MF-EDM process was established as shown in Fig. 3, Fig. 3a shows the schematic diagram of the whole experimental setup including MF-EDM and aerosol collection setup. Particularly, Fig. 3b presents the schematic diagram of aerosol sampling setup and Fig. 3c illustrates the flowchart of aerosol sampling process. A transparent plastic cover was placed to cover discharge machining area between the electrodes and workpiece as well as immersed in the dielectric fluid in order to enclose the entire aerosol emissions. Two small holes are made in the cover to connect with fresh air to compensate the air sucked by the pump. There is an opening under the small hole to tightly connect with the pump through the tubing. The emitted gas with aerosols from MF-EDM process of $HVF - SiC_p/Al$ were gathered in the transparent plastic cover and driven to pass through the soft tube into the glass bottle by air sampler with an internal pump. The aerosol emissions can be collected by PVC filter.

In details, a (SKC PCXR8) Universal Air Sampler with cyclone (as shown in Fig. 3b) was used to drive the air flowing and collect the samples of aerosol emission via filter paper, which has ability to filter non-inhalable particles above 5 μm. A soap bubble meter was used to calibrate the velocity of gas for the sampler both before and after sampling. In this experiment, the velocity of gas was set to be 3L/min all the time. Aerosol emissions was mightily pulled through a PVC filter with diameter of 37 mm and pore size of 5 μm, and particles in the aerosol emissions would be attached to the filter paper. The sampling duration keeps continuous throughout the whole MF-EDM process for each experimental set. A sensitive electronic balance (acc. 100 μg) was used to measure the filter paper weight before and after each experiment. Equation (3) was used to calculate the concentration of aerosols (C_A) (Mathew et al., 2010b).

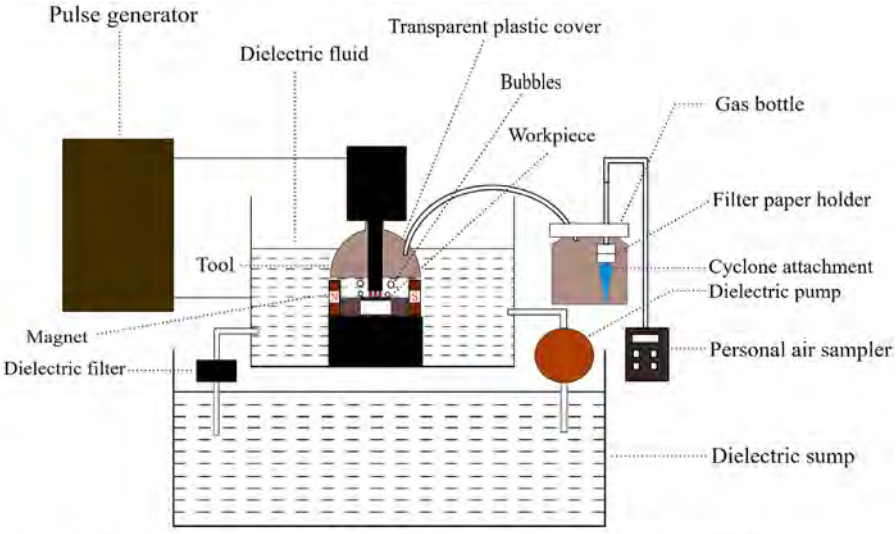

(a) Schematic diagram of experimental setup for aerosol sampling in MF-EDM process

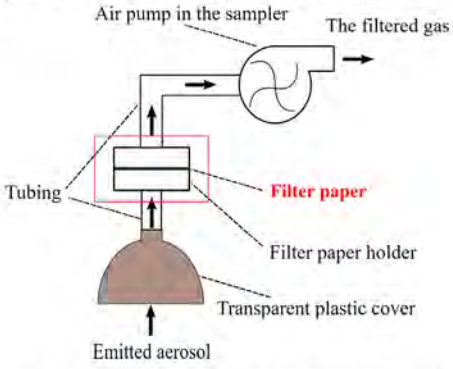

(b) Schematic diagram of aerosol sampling setup

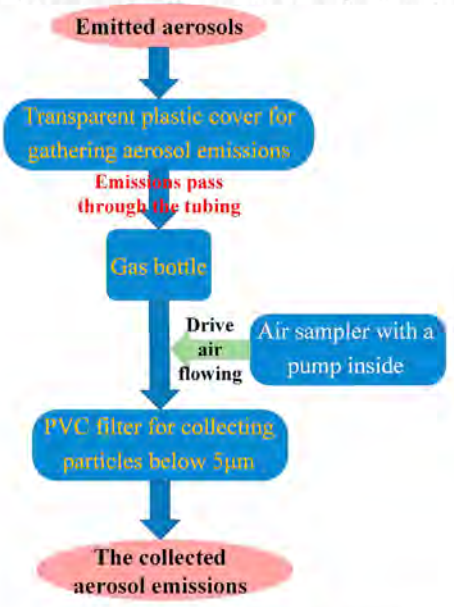

(c) Flowchart of aerosol sampling process

Fig. 3. Schematic diagram of experimental setup for aerosol sampling in MF-EDM process.

$$C_A = \frac{(W_b - W_a) \times 1000}{t_s \times v} \quad (3)$$

where

C_A – Concentration of aerosols (mg/m^3)
W_a – Weight of filter paper before sampling (mg)
W_b – Weight of filter paper after sampling (mg)
v – Sampling speed (lpm)
t_s – Sampling duration (min)

2.5.4. Surface integrity

The machined workpiece were made into samples with a size of 10mm × 10mm. The micro cracks, remelted debris, and surface voids of all samples were tested and analyzed respectively by thermal field emission scanning electron microscope whose model is JSM-7600F with high spatial resolution and high scan speed. Leica DVM6, a high field depth digital microscope, was used to shot and analyze the three dimensional surface topography of machined workpiece.

3. Results and discussion

3.1. MRR

The change tendency of MRR for 45% and 65% SiC_p/ Al under different experimental parameters (I, B, T_on and T_off) via a series of experimental groups can be observed in Fig. 4a. The MRR value represents the machining efficiency and machining emissions from the workpiece material of MF-EDM process. Overall, the machining efficiency of the two materials has similar change tendency, whereas the machining efficiency of 45% volume fraction SiC_p/ Al is generally better than that of 65% SiC_p/Al at the same experimental group number. Fig. 5a also shows the same result that MRR of 45% SiC_p/Al is a little better than that of 65% SiC_p/Al even under the variation of four input process parameters. This is mainly attributed to that the ceramic-reinforced component (SiC_p) in aluminum-based materials with the low electrical conductivity prevents normal discharge and debris movement between the workpiece and the tool electrode so as to negatively affect next normal discharge and the materials removal. Therefore, the more SiC particle fractions contained in SiC_p/Al, the harder it is to process using EDM.

A detailed analysis of the main effect and its delta of each process parameter, including I, B, T_on, and T_off, on MRR of 45% and 65% SiC_p/Al is presented as shown in Figs. 5a and 6a. Delta is the gap between the lowest and highest response value for each factor and is used to reflect the relative effect of each parameter on the response. Compared with these curves of 5a and 6a, it can be found that among the four parameters, the pulse current has most significant impact on the machining efficiency of 45% and 65% SiC_p/Al. With the increase of the pulse current, the erosion of the material becomes more intense through high discharge energy flowing into the workpiece material so that the machining efficiency is sharply improved. The MRR of two materials both slightly fluctuate with the increase of T_on value and T_off value, and it indicates the best effect when the value of T_on is 150 μs. This may be because too small T_on and T_off values will cause insufficient pulse discharge, material erosion as well as deionization process in the machining cycle, while large T_on and T_off values are beneficial to not only enduring discharge energy to remove material but also debris having enough time to be taken away from the processing area in time. However excessive

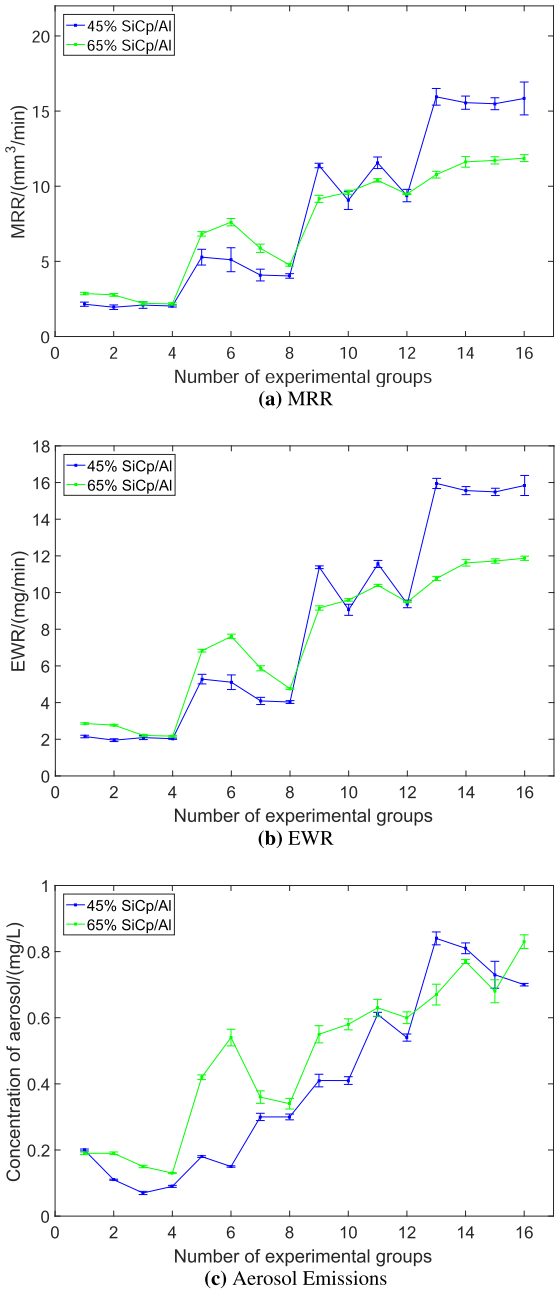

Fig. 4. Comparison of 45% and 65% SiC_p/Al via a series of experimental groups: (a) MRR; (b) EWR; (c) Aerosol emissions.

T_off value goes against the improvement of machining efficiency due to lacking sufficient pulse discharge erosion time. Additionally, magnetic field has a little positive impact on MRR. Particularly, in some range magnetic field intensity has positive correlation with machining efficiency. The main reason is that the increase of magnetic field intensity could make the discharge channel more concentrated to improve discharge energy efficiency as well as contributing to Al debris pulled away from electrodes' gap by Lorenz force. This also proves that higher volume fraction of SiC particles in SiC_p/Al becomes harder to machine even under the effect of assisted magnetic field. Assisted magnetic field could affect the motion of charged particles and help the debris be taken away from the discharge gap via generating Lorentz force. The formation of molten

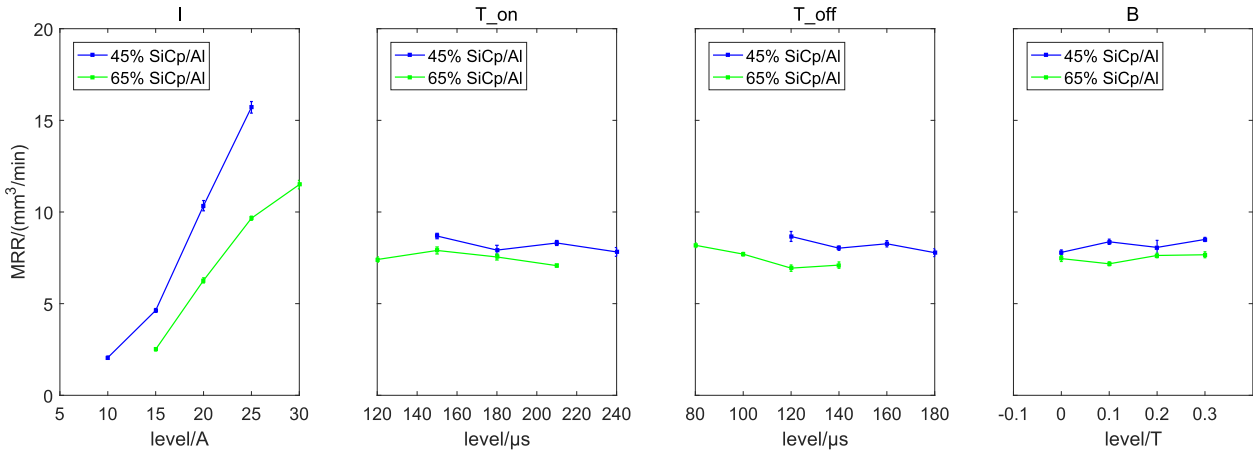

(a) MRR

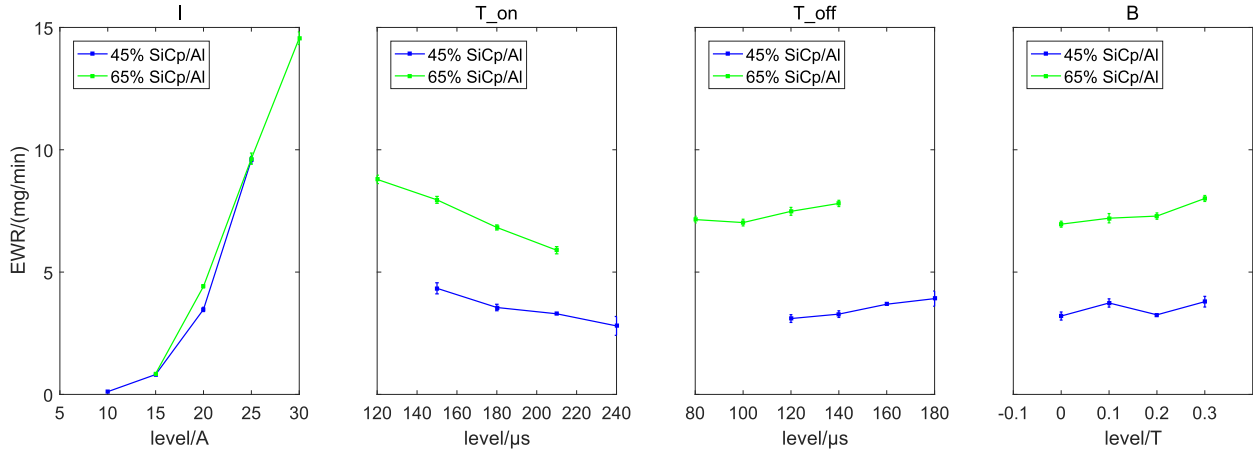

(b) EWR

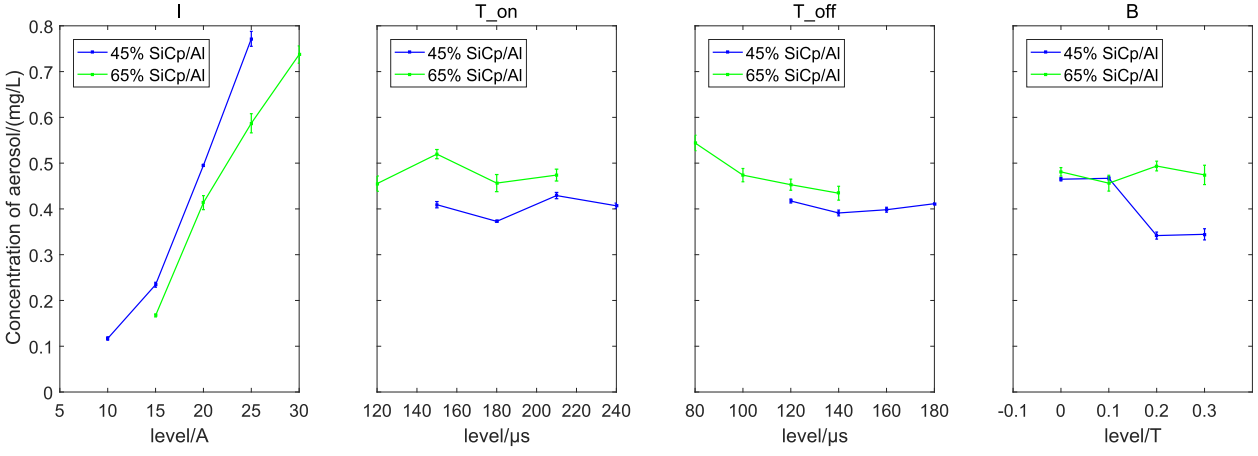

(c) Aerosol Emissions

Fig. 5. Comparison of the main effect of each process parameter on 45% and 65% SiC_p/Al: (a) MRR; (b) EWR; (c) Aerosol emissions.

pool can be also boosted due to the greater plasma pressure near the molten pool which increased the possibility of material eruption under the effect of magnetic field. So the efficiency of material removal and ablation can be developed while The deposition of debris can be reduced during the MF-EDM process.

Assisted magnetic field could affect the motion of charged particles and help the debris be taken away from the discharge gap via generating Lorentz force (Zhang et al., 2020a, 2020c). The formation of molten pool can be also boosted due to the greater plasma pressure near the molten pool which increased the possibility of material eruption under the effect of magnetic field (Heinz et al., 2011). So the efficiency of material removal and ablation can be developed while the deposition of debris can be reduced during the MF-EDM process.

3.2. EWR

Fig. 4b shows the variation of EWR for 45% and 65% SiC_p/ Al under different experimental parameters (I, B, T_on, and T_off) via a series of experimental groups. The EWR value indirectly reflects the quantity of machining emissions from the electrode material in the MF-EDM process. Overall, the EWR of the two materials has similar change tendency, whereas the EWR of 65% volume fraction SiC_p/ Al is much higher than that of 45% SiC_p/Al at the same experimental group number. Fig. 5b also shows the same result that EWR of 45% SiC_p/Al is much better than that of 65% SiC_p/Al even under the variation of four input process parameters. Since the melt point of ceramic-reinforced component (SiC_p) is much higher than that of aluminum substrate, SiC_p/Al containing more volume fraction of SiC particles requires more pulse discharge energy to be melted and vapored, while higher input energy inevitably results in larger electrode erosion (EWR). That is the main reason that compared to 45% SiC_p/Al, EWR and machining emissions of 65% SiC_p/ Al are much greater.

Figs. 5b and 6b illustrate the main effect and its delta of each process parameter, on EWR of 45% and 65% SiC_p/Al. Compared with these curves of Figs. 5b and 6b, it can be found that among the four parameters, the I and T_on are two most significant factors on the EWR of HVF – SiC_p/Al. With the increase of the pulse current, the erosion of electrode material becomes more intense through high discharge energy flowing into the electrode material, which leads to dramatic development of EWR. On the contrary, the electrode loss gradually decreases as the T_on time rises. The main fact is that the increase of T_on value lengthens the proportion of discharge time in one pulse discharge cycle, which contributes to the formation of the protective film on the electrode surface as well as the reduction of electrode loss. Opposite to the effect of T_on value on EWR, the electrode loss goes up slightly with the increase of T_off value. Because the increase of the T_off value to some extent will block and damage the generation of protective film on the electrode surface via extending deionization process in one pulse discharge cycle. Similarly, to increase assisted magnetic field intensity leads to a little decrease of EWR. Since the concentrated discharge energy increases the energy utilization efficiency and MRR under the effect of magnetic field, it also could fasten the fracture of protective film on the electrode surface via excessive discharge energy. Even so, as shown in Fig. 6b, the influence of magnetic field intensity on electrode loss is relatively weak, particularly for 45% SiC_p/ Al (relatively low volume fraction SiC_p/Al).

EDM is a kind of precision machining with some harmful exhausted emissions, and EWR directly affects the machining accuracy and sources of hazardous products and air pollution including Carbon, Silicon, Aluminum, and Copper oxide in the MF-EDM process of HVF – SiC_p/Al. From above analysis, it can be revealed that the EWR sharply goes up with the increase of volume fraction of SiC particles, and the reason for this increase is that tool materials have to take additional material loss due to the ablation behavior of SiC (Mahdavinejad et al., 2005; Saxena et al., 2018). These results confirm that the workpiece materials and its properties have a significant effect on the performance of EWR. Besides, influences of input discharge energy on EWR show more significant than that of assisted magnetic field intensity. The selection of small pulse current and pulse off-time, large pulse on-time, and appropriate magnetic field intensity could achieve the low EWR especially for HVF – SiC_p/Al. which could contribute to guide the optimization of MF-EDM process of HVF – SiC_p/Al.

3.3. Aerosol emissions

Fig. 4c shows the variation of concentration of aerosol emissions for 45% and 65% SiC_p/Al under different experimental parameters (I, B, T_on, and T_off) via a series of experimental groups. The value of aerosol emissions directly reflects the quantity of machining emissions and effect of MF-EDM process for the environment. Overall, although aerosol emission of 65% volume fraction SiC_p/Al is just a little higher than that of 45% SiC_p/Al at the same experimental group number, the aerosol emissions of two materials has similar change tendency and little difference. According to the main effect and its delta of each process parameter on aerosol emissions of 45% and 65% SiC_p/Al as shown in Figs. 5c and 6c, it can be found that among the four parameters, the pulse current is the most significant factors on the aerosol emissions of HVF – SiC_p/Al. With the increase of the pulse current, much more intensive discharge energy flowing into two electrodes leads to much larger and severer erosion of electrode and HVF – SiC_p/Al material. This process could generate dramatic emissions of aerosol. Additionally, assisted magnetic field could contribute to slightly reduce the concentration of aerosol emissions when magnetic field intensity ranges from 0.1 to 0.2T. This is mostly attributed to the fact that appropriate magnetic field could increase discharge energy utilization efficiency (Ming et al., 2019) to balance the materials removal and aerosol emissions.

In order to analyze the composition of emitted aerosols from MF-EDM of HVF – SiC_p/Al, some typical samples (Nos.6, 11, and 16 in Table 4) of 65% SiC_p/Al were selected to further investigate EDS (Energy Dispersive Spectrometer) analysis of surface emblements. As illustrated in Fig. 7a, b, and 7c, no matter in which samples, three highest element content of emitted aerosols are all carbon, oxygen, and silicon, taking up more than 80% of the whole sampled aerosols.

On the other hand, as shown in Fig. 7d, although different aerosol samples were selected, distribution of elements in the aerosol emissions is exactly similar. It reveals that compositions of aerosol emissions from MF-EDM process of HVF – SiC_p/Al are the same level and hazardous to the environment and operators' health even under different process parameter conditions.

Section 3.5 presents more analysis on the effects of the aerosol emissions and their hazardous derivatives on the operators' health and environmental pollution.

3.4. Surface integrity

In order to analyze the surface integrity of MF-EDM process of HVF – SiC_p/Al, some samples of 65% SiC_p/Al were selected to further investigate surface micro structure and surface topography. Figs. 8 and 9 present three-dimensional surface topography of two different areas of Sample Nos.6 and 12 in Table 4 for the EDM process without and with magnetic field (B = 0.2T). The highest peaks in two areas of MF-EDM process are 3.700 μm and 4.090 μm, while the highest peaks in two areas of EDM process are 7.590 μm and 6.360 μm. Compared with the 3D surface of EDM, discharge crater is much smaller and more uniform, placing tightly on the surface of MF-EDM. Moreover, variation of peak-valley in the 3D surface of EDM fluctuates more severely than that of MF-EDM. Thus above results directly reveal that surface roughness of MF-EDM process provides much smoother surface roughness than EDM process. The main reason is that assisted MF could not only create smaller and more uniform discharge spots to generate uniform discharge crater, but also improve the stability of plasma channel to make crater locations intensive.

Figs. 10 and 11 demonstrate SEM surface micro structure of Sample Nos.6 and 12 in Table 4 for the EDM process without and with magnetic field (B = 0.2T). In the condition of × 2000, lots of voids and cracks can be obviously found on the machined surface of EDM process. Zooming in the areas of these voids and cracks (×

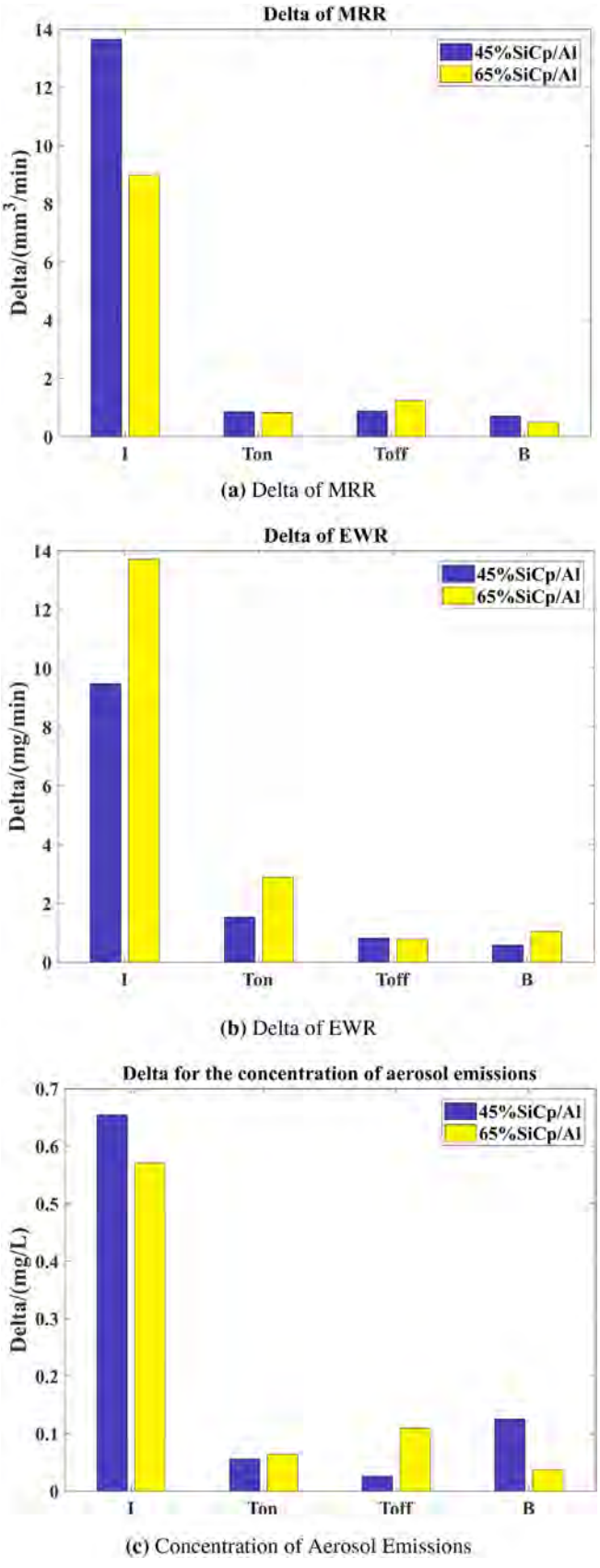

Fig. 6. Comparison of the main effect delta of each process parameter on 45% and 65% SiC_p/Al: (a) MRR; (b) EWR; (c)Delta for the Concentration of Aerosol emissions.
P.S. Delta is the difference between the highest and lowest average response values for each factor. Minitab Software assigns ranks based on Delta values; Rank 1 to the highest Delta value, Rank 2 to the second highest, and so on, to indicate the relative effect of each factor on the response.

5000), the micro defects, large and dense voids as well as long, wide, deep cracks, can be distinctly exposed. In contrast, even in the condition of × 5000, the sample surface with external magnetic field intensity of 0.2T which makes the discharge energy uniform, just shows a few micro voids with small size and no significant micro cracks (only short, narrow, and shallow cracks). So this also proves that assisted magnetic field contributes to significantly improve the surface integrity of EDM process of HVF − SiC_p/Al.

Surface integrity and microstructure are one of important machining performance indicators, which directly affect mechanical properties of machined surface by EDM process (Ming et al., 2020). Above results demonstrated that even though assisted magnetic field contributes to significantly improve the surface integrity with a few micro cracks and voids, it can't completely relief the thermal damages on the machined surface due to electrical sparks discharge process and the brittleness of SiC ceramic.

3.5. Environmental impact

During the EDM process, the main emissions are particles of Carbon, Silicon, Aluminum, Copper and their oxides. About 80% emissions consist of Carbon and Silicon oxide, and about 20% are Aluminum and Copper oxide (See Fig. 12).

Carbon mainly generated by SiC particles and decomposition of kerosene oil (a high molecular hydrocarbon with strong volatility) during the MF-EDM process, while oxygen comes from air and decomposition of kerosene oil. Carbon emissions contains CO_2, CO and carbon particles. CO_2 is the major greenhouse gas emitted by the activity of human. It accounted for about 81.3% of all green house emissions from human all over the United States in 2018 (EPA, 2018). Over emission of greenhouse gas leads global warming, which causes serious environmental problems, such as sea level rise, abnormal distribution, and frequent flooding and drought. CO can threaten human's health by reducing oxygen delivery to the body's organs and tissues, even capable of causing death at very high levels (Masoudi and Gerami, 2017). Carbon particles have important impact on both the environment and public health. To the environment, carbon particles can directly absorb the radiation of solar or terrestrial which contributes to the warming of the atmosphere. It also darkens the surface of snow and ice, thereby increasing melting (EPA, 2012). To the human body, breathing carbon particles can decrease lung function, develop emphysema, even cause lung cancer (Leonard et al., 2020). Carbon particles are also associate with PM2.5 fraction, which leads adverse human respiratory and cardiovascular effects, and estimates to cause millions of premature deaths every year all over the world (EPA, 2012).

Silicon completely comes from SiC particles, accounting for almost 20% of the whole sampled aerosols, which probably exists in the form of SiO_2 particles emitted into the air. If EDM operators long-term inhales this SiO_2 particles via the aerosol emissions from EDM's exhaust, they easily suffer from lung disease. When silica build up in the respiratory tract and lungs, they lead to hard breathing, such disease is called silicosis. Silicosis is one of the utmost occupational diseases in the world prompting lung fibrosis (Leung et al., 2012), which increases the odds of getting tuberculosis, chronic bronchitis, chronic obstructive pulmonary and lung cancer.

Additionally, aerosol emissions contain aluminum and copper from Al substrate and copper electrode, which together take up about 15% of the whole sampled aerosols. Excessive inhaling aluminum and copper particles is also pretty harm to operators'

Table 3
Experimental results of 45% volume fraction.SiC_p/Al

No.	I	T_on	T_off	B	MRR	EWR	Aerosol Emissions
	(A)	(ms)	(ms)	(T)	(mm^3/min)	(mg/min)	(mg/L)
1	10	150	120	0	2.15	0.22	0.20
2	10	180	140	0.1	1.95	0.08	0.11
3	10	210	160	0.2	2.09	0.08	0.07
4	10	240	180	0.3	2.03	0.06	0.09
5	15	150	140	0.2	5.28	1.13	0.18
6	15	180	120	0.3	5.11	0.99	0.15
7	15	210	180	0	4.09	0.63	0.30
8	15	240	160	0.1	4.03	0.50	0.30
9	20	150	160	0.3	11.38	4.69	0.41
10	20	180	180	0.2	9.06	3.66	0.41
11	20	210	120	0.1	11.56	3.05	0.61
12	20	240	140	0	9.38	2.49	0.54
13	25	150	180	0.1	15.95	11.31	0.84
14	25	180	160	0	15.56	9.48	0.81
15	25	210	140	0.3	15.49	9.42	0.73
16	25	240	120	0.2	15.84	8.14	0.70

Table 4
Experimental results of 65% volume fraction.SiC_p/Al

No.	I	T_on	T_off	B	MRR	EWR	Aerosol Emissions
	(A)	(ms)	(ms)	(T)	(mm^3/min)	(mg/min)	(mg/L)
1	15	120	80	0	2.86	1.35	0.19
2	15	150	100	0.1	2.77	0.81	0.19
3	15	180	120	0.2	2.21	0.69	0.15
4	15	210	140	0.3	2.17	0.54	0.13
5	20	120	100	0.2	6.83	5.51	0.42
6	20	150	80	0.3	7.61	5.77	0.54
7	20	180	140	0	5.87	3.79	0.36
8	20	210	120	0.1	4.76	2.60	0.34
9	25	120	120	0.3	9.16	11.70	0.55
10	25	150	140	0.2	9.60	10.29	0.58
11	25	180	80	0.1	10.39	8.80	0.63
12	25	210	100	0	9.48	7.76	0.6
13	30	120	140	0.1	10.77	16.60	0.67
14	30	150	120	0	11.62	14.94	0.77
15	30	180	100	0.3	11.72	14.02	0.68
16	30	210	80	0.2	11.87	12.68	0.83

health. Aluminum toxicity may hurt human's bones, brain and nervous system. Chronic copper toxicity may endanger human's liver as well as nervous system (National-Research-Council, 2000).

The above analysis has shown that aerosol emissions from EDM process are extremely harmful for both the operators' health and the nature environment. Hence, the optimization of ED machining HVF – SiC_p/Al is urgently demanded in order to reduce the emissions and achieve a cleaner and safer production process.

4. Optimization

To achieve the better sustainable performance of MF-EDM process of HVF – SiC_p/Al, a multi-objective optimization algorithm is employed to optimize this complex process through combining BPNN and GAQPSO. It takes above MF-EDM experiment results as input and gives a non-dominance set as output with simultaneously maximum MRR, minimum EWR, and minimum concentration of aerosol emissions (Pareto-optimal) as output.

4.1. Multi-objective pareto-optimal

Since there are several objectives for each solution, every objective should be compared separately for solutions to get optima results. The optimal outputs are contained in a set, where no element in the set is superior to another in all objectives. More precisely, if solution A is better than B in all areas, we call that A *dominates* B. If A is better than B in some areas but worse than B in some others, A and B are called *non-dominance solutions*. The optimum solutions for multi-objective optimization is a set in which every two solution are non-dominance to each other. Such optimal solutions are called *Pareto-optimal*.

4.2. GAQPSO with BPNN

GAQPSO uses wave function from quantum physics rather than speed from classic physics (in PSO) to update the particles in the algorithm (Sun et al., 2011). The particles states are described by wave function with δ-potential well. Moreover, a local factor is determined by Gaussian distribution. It helps to jump out from local best results hence to achieve global optimization. The particle states can be described as follows:

$$U_i(t+1) = \phi \cdot Pb_i(t) + (1-\phi) \cdot Gb(t) \tag{4}$$

$$U_i'(t+1) = N(U_i(t+1), |m_i(t) - Pb_i(t)|) \tag{5}$$

$$X_i(t+1) = U'_i(t+1) \pm \alpha \cdot |m_i(t) - X_i(t)| \cdot \ln(1/u) \tag{6}$$

$$m_i(t) = \frac{1}{N}\sum_{i=1}^{N} Pb_i(t). \tag{7}$$

where α is coefficient of Contraction-Expansion generally taken as $\alpha < 1.781$, it is usually a linear decreasing value or a constant. *Gb* is the global best state (*gbest*) of all the particles, Pb_i is the personal or local best state (*pbest*) of the *i*th particle. $\phi = c_1 \cdot r_1/(c_1 \cdot r_1 + c_2 \cdot r_2)$, where c_1 and c_2 are two coefficient argument usually taken as 2, r_1 and r_2 are two random values on (0,1). U_i is the original local state of every particle, and U'_i is the new local state with Gaussian distribution *N*. *u* is random on (0,1). Mean best value m_i is the average of all the *pbest* of the particles.

BPNN is used to generate a model, which will be used as a fitness function of the GAQPSO algorithm. It is an efficient version of neural network, which calculates the weights to improve the network until it is able to perform the task for which it is being trained. In BPNN, the output errors are linked back to the input until the algorithm meets the maximum iteration or minimal error.

4.3. Model settings

In this work, the particles of GAQPSO are used as simulated experiment trails. Each particle has 4 dimensions, which stand for the value of I, T_on, T_off and B. Every particle has 3 criteria as fitness values: EWR, MRR and aerosol emissions. A model of BPNN is created with 4 inputs, 3 outputs and a hidden layer with 4 neurons. The fitness values of each particle is calculated by the BPNN. Every particle has a *pbest* state. For all the particles, a non-dominance set is used for *gbest* state. To keep diversity of the results, crowd distances are calculated for the points in the non-dominance set. When the size of gbest set is over maximum value, fresh non-dominance point will substitute the point with nearest crowding distance. The algorithm flow chat is given in Fig. 13.

4.4. Optimization results discussion

4.4.1. Optimization results of 45% volume fraction SiC_p/Al

Fig. 14 presents the optimal Pareto surface of global best set for

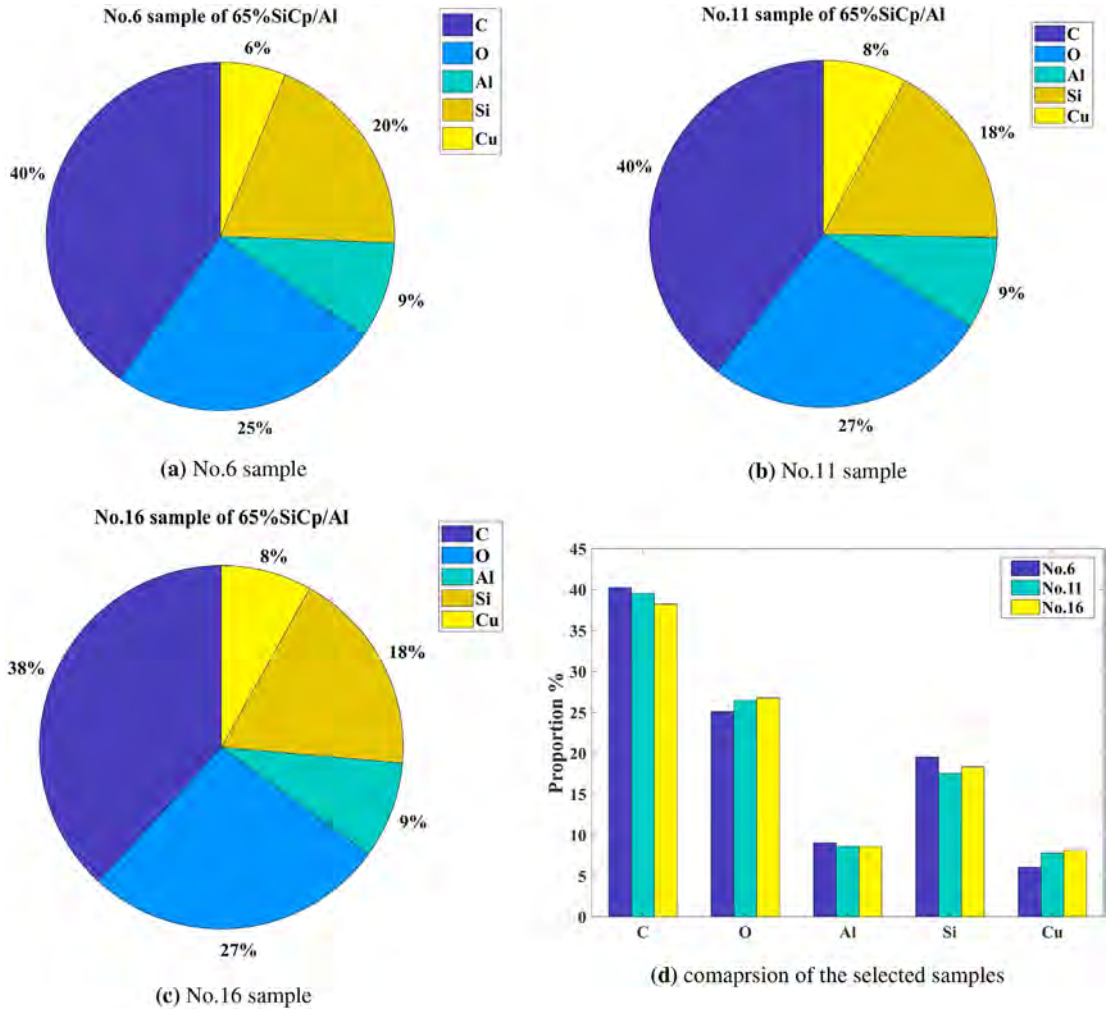

Fig. 7. EDS quantitative analysis of surface elements.

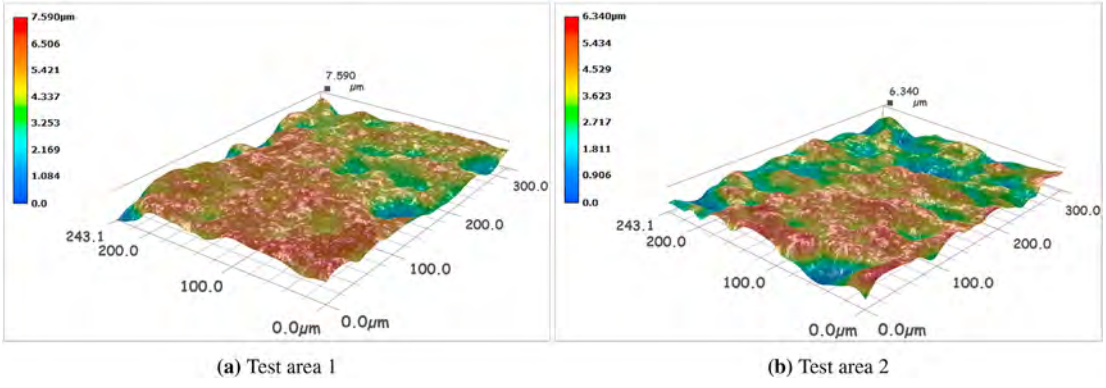

Fig. 8. Three-dimensional surface topography of EDM without magnetic field (No.12 in Table 4): (a) Test area 1; (b) Test area 2.

45% volume fraction SiC_p/Al, the points in the figure are 16 selected optimized results, which contains minimal and maximum MRR, EWR and Emission values as well as some compromised points. Table 5 lists the 16 optimized results. The values of MRR range from 2.15 to 16.86 (mm^3/min); the values of EWR range from 0.054 to 9.04 (mg/min); the values of aerosol emission range from 0.087 to 0.67 (mg/L).

The results holding minimum EWR and maximum MRR values in both Table 3 and Table 5 can be viewed as typical cases in our optimization. No.4 of Table 3 and No.2 of Table 5 hold minimal EWR values in their tables. Comparing the two results, EWR is decreased by 10% (from 0.06 to 0.054) while the MRR is increase by 5.9% (from 2.03 to 2.15), however emission is increased by 4.4% (from 0.09 to 0.094) as payback, the results are non-dominance results to each other. No.13 of Table 3 and No.16 of Table 5 hold maximum MRR values in their tables. Comparing the two results, MRR is increase

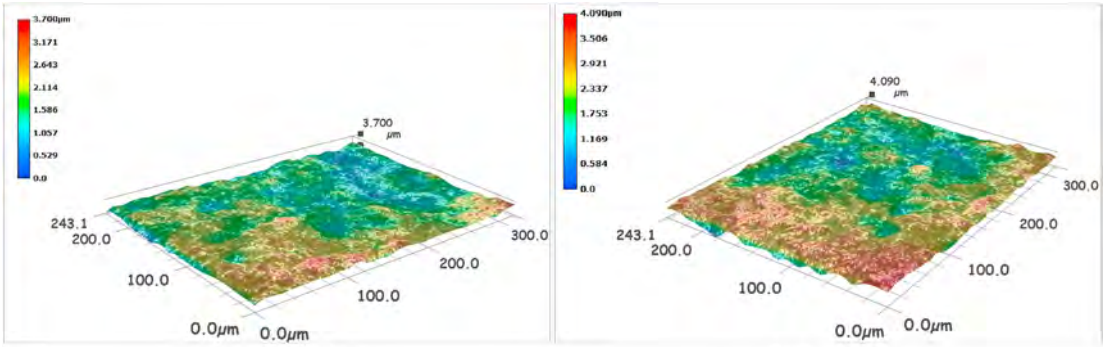

(a) Test area 1 (b) Test area 2

Fig. 9. Three-dimensional surface topography of EDM with magnetic field (No.6 in Table 4): (a) Test area 1; (b) Test area 2.

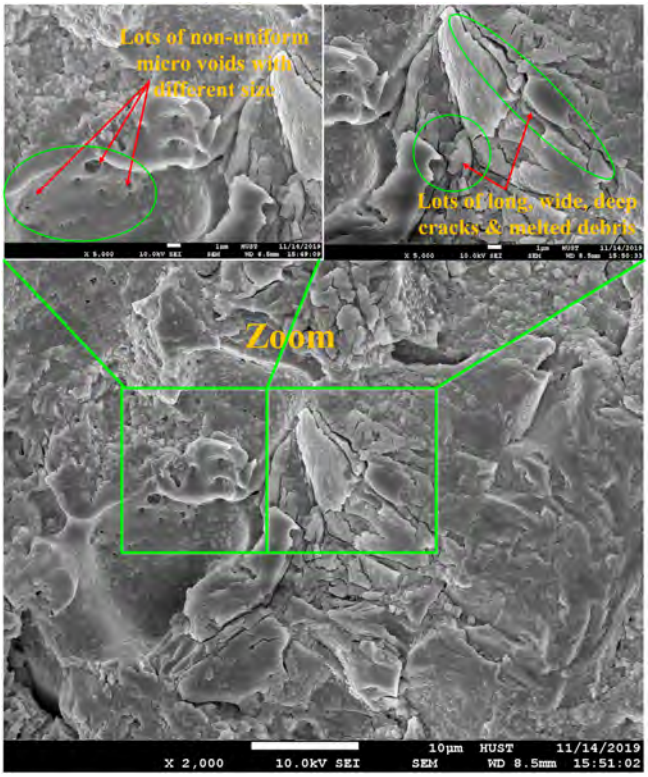

Fig. 10. SEM surface topography of EDM without magnetic field (No.12 in Table 4).

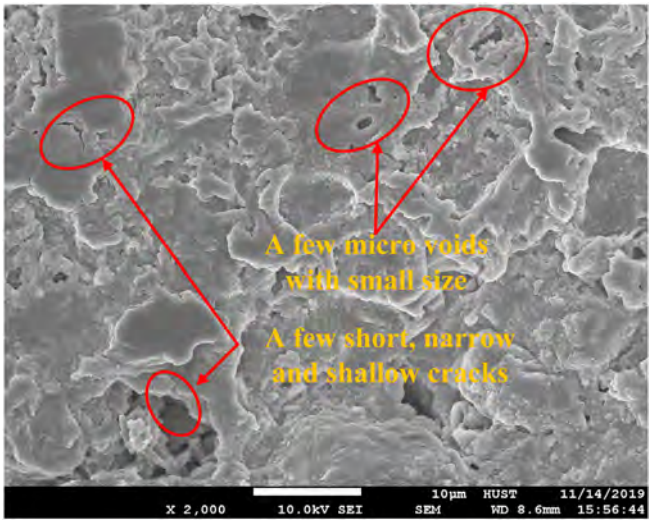

Fig. 11. SEM surface topography of EDM with magnetic field (No.6 in Table 4).

by 5.7% (from 15.95 to 16.86) while the EWR is decreased by 25% (from 11.31 to 9.04) and the aerosol emission is decreased by 31% (from 0.84 to 0.64). It means that No.16 of Table 5 dominates No.13 of Table 3. It can been seen that at lower EWR side, the optimization improves both EWR and MRR values with paying a small amount of aerosol emission as price; and at higher MRR side, the optimization provides a better result.

Over all the 16 optimized results, the mean value of MRR, EWR and aerosol emissions are 8.72 (mm^3/min), 3.14 (mg/min) and 0.34 (mg/L) respectively. For the 16 experimental results, the mean value of MRR,EWR and aerosol emissions are 8.18(mm^3/min), 3.50(mg/min), 0.40(mg/L) respectively. MRR is increased by about 6.6%, EWR is decreased by about 10% and aerosol emissions are decreased by about 15%. It shows that the optimization can provide better design options of process parameter combinations.

4.4.2. Optimization results of 65% volume fraction SiC_p/Al

Fig. 15 presents the optimal Pareto surface of global best set for 65% volume fraction SiC_p/Al, the points in the figure are 16 selected optimized results, which contains minimal and maximum MRR, EWR and aerosol emissions values as well as some compromised points. Table 6 lists the 16 optimized results. The values of MRR range from 3.66 to 12.18 (mm^3/min); the values of EWR range from 0.41 to 14.96 (mg/min); the values of aerosol emissions range from 0.078 to 0.87 (mg/L).

The results holding minimum EWR and maximum MRR values in both Tables 4 and 6 can be viewed as typical cases in our optimization. No.4 of Table 4 and No.1 of Table 6 have minimum EWR results in each table. Comparing the two results, MRR is increase by 41% (from 2.17 to 3.66) while EWR is decreased by 24% (from 0.54 to 0.41) and the aerosol emission is decreased by 40% (from 0.13 to 0.078). It means that No.1 of Table 6 dominates No.4 of Table 4. No.16 of Table 4 and No.16 of Table 6 contains maximum MRR results in each table. Comparing the two results, MRR is increase by 2.5% (from 11.87 to 12.18) while EWR is slightly decreased and the aerosol emission is increased by 4.6% (from 0.83 to 0.87), the two results are non-dominance to each other. It can be seen that at higher MRR side, the optimization improves both EWR and MRR values with paying some aerosol emission as price, however at lower EWR side, the optimization provides a better result.

Over all the 16 optimized results, the mean value of MRR, EWR

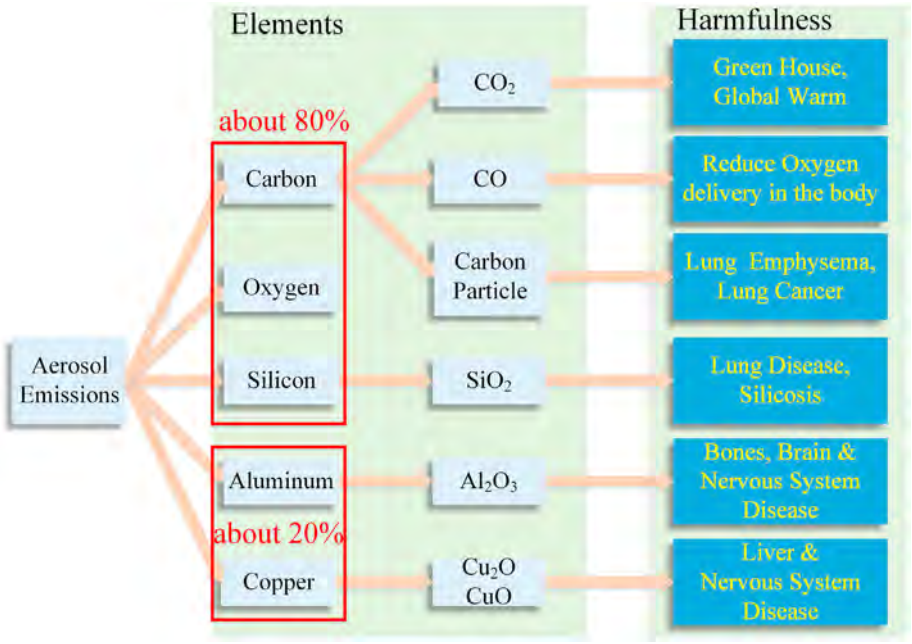

Fig. 12. Harmfulness of aerosol emissions.

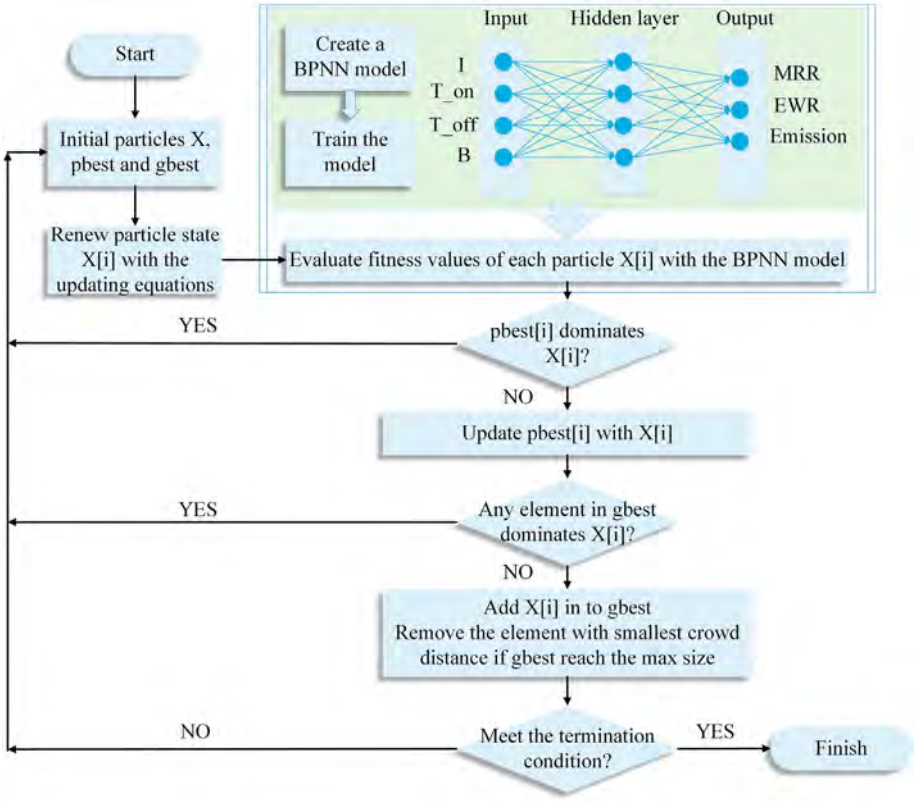

Fig. 13. The flow chat of GAQPSO-BPNN algorithm.

and aerosol emissions are 7.89mm^3/min, 6.95 (mg/min) and 0.43 (mg/L) respectively. For the 16 experimental results, the mean value of MRR,EWR and Emissions are 7.48mm^3/min, 7.37(mg/min), 0.48(mg/L) respectively. MRR is increased by about 5.5%, EWR is decreased by about 5.7% and aerosol emissions are decreased by about 10%. All the above have demonstrated that the optimization can provide better design options of process parameter combinations.

5. Conclusion

In this paper, magnetic field assisted electrical discharge

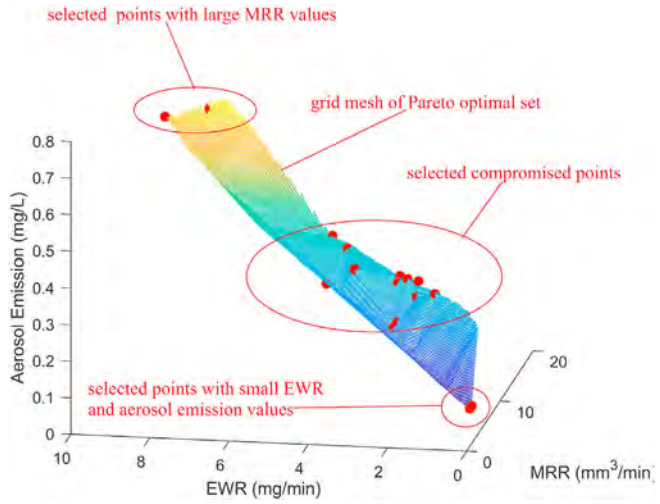

Fig. 14. Optimal Pareto surface for 45% volume fraction.SiC_p/Al

Table 5
Selected optimization results of 45% volume fraction.SiC_p/Al

No.	I	T_on	T_off	B	MRR	EWR	Aerosol Emissions
	(A)	(ms)	(ms)	(T)	(mm^3/min)	(mg/min)	(mg/L)
1	10	176	137	0.2	2.15	0.054	0.094
2	10	158	137	0.3	2.13	0.10	0.087
3	15	220	144	0.1	6.72	1.37	0.33
4	18	176	132	0.3	6.86	2.42	0.23
5	16	160	131	0.2	6.96	2.35	0.25
6	13	230	136	0.1	7.43	1.88	0.31
7	17	223	131	0.0	7.63	1.86	0.35
8	16	217	135	0.1	8.13	2.18	0.35
9	16	193	134	0.1	8.30	2.44	0.34
10	15	213	126	0.0	8.59	2.41	0.35
11	19	162	148	0.2	8.92	3.58	0.36
13	20	153	127	0.3	9.54	4.35	0.31
14	19	193	123	0.1	10.87	3.93	0.39
12	19	235	121	0.2	11.98	4.40	0.40
15	25	216	121	0.3	16.42	7.88	0.67
16	25	174	127	0.3	16.86	9.04	0.64

machining of HVF – SiC_p/Al was proposed to improve the sustainable machining performance. Two groups of Taguchi experiments were carried out to completely investigate MRR, EWR, aerosol emissions, and surface integrity of SiC_p/Al composites with 45% and 65% volume-fraction. Moreover, BPNN-GAQPSO algorithm was introduced to optimize the MF-EDM process of HVF – SiC_p/Al composites in an economically and environmentally manner. Main contribution of this can be concluded as follows:

1. The pulse current is the most significant factors affecting the MRR, EWR, and aerosol emissions of MF-EDM process of HVF – SiC_p/Al. Magnetic field assisted technology significantly develops the surface integrity of the EDM process of HVF – SiC_p/Al, while it just slightly contributes to improve its sustainable performance with reductions in EWR and aerosol emissions whereas increase of MRR when intensity of MF is in the range of 0.1T–0.2T.
2. Aerosols generated by MF-EDM process of HVF – SiC_p/Al mainly contain carbon, oxygen, silicon, aluminum, and copper, whereas carbon, oxygen, and silicon taking up more than 80% of the whole sampled aerosols mostly exist in the form of SiO_2 and carbon particles, which are harmful to operators' health and ecological environments.
3. BPNN-GAQPSO algorithm is introduced to provide optimal machining parameters. Compared to the average data of experiment: for 45% SiC_p/Al, the average optimal solutions of EWR, and aerosol emission were decreased by about 10% and 15% whereas MRR was increased by about 6.6%; for 65% SiC_p/Al, the average optimal solutions of EWR, and aerosol emission were decreased by about 5.7% and 10% whereas MRR was increased by 5.5%. The typical results comparison also shows that the optimization algorithm provides improved results. The provided optimized machining parameters can notably guide EDM process in an economic and environmental way, and satisfy sustainable manufacturing needs as well.

In the future, we will focus on the following research points to chase the challenges in the green and sustainable manufacturing process for electrical discharge machining advanced materials.

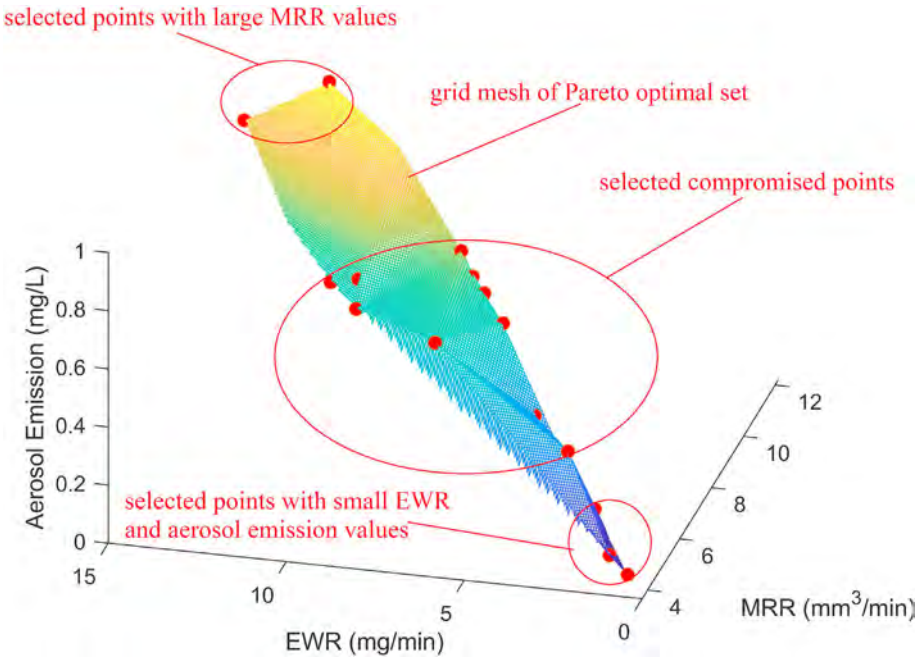

Fig. 15. Optimal Pareto surface for 65% volume fraction.SiC_p/Al

Table 6
Selected optimized results for 65% volume fraction.SiC_p/Al

No.	I	T_on	T_off	B	MRR	EWR	Aerosol Emissions
	(A)	(ms)	(ms)	(T)	(mm^3/min)	(mg/min)	(mg/L)
1	19	196	97	0.1	3.66	0.41	0.078
2	19	196	97	0.0	4.27	1.19	0.081
3	20	206	82	0.1	5.61	2.20	0.11
4	21	207	99	0.1	5.69	2.99	0.29
5	20	207	87	0.0	6.52	3.36	0.16
6	21	201	97	0.0	6.97	4.50	0.28
7	25	153	109	0.1	7.01	7.32	0.49
8	23	209	87	0.1	7.98	5.85	0.49
9	23	129	136	0.1	8.12	10.04	0.48
10	23	207	102	0.1	8.58	6.64	0.53
11	23	209	122	0.1	8.81	7.07	0.56
12	23	209	116	0.1	9.18	7.56	0.61
13	28	133	85	0.2	9.54	11.65	0.58
14	29	123	132	0.1	10.03	12.85	0.57
15	30	148	134	0.1	12.06	14.96	0.71
16	28	195	134	0.0	12.18	12.62	0.87

i. Based on deep learning technique, intelligent EDM process shall be the future developing trend to improve its suitability and environmental friendship, which is very important to determine the best combination of processing parameters in the EDM of new advanced materials.
ii. Hybrid EDM processes possess comprehensive advantages of different process techniques, and they provide more opportunities and potentials for efficiently machining advanced materials with the reduction of energy consumptions. Thus in the future we will continue to develop a new hybrid EDM technique for green and sustainable manufacturing.

CRediT authorship contribution statement

Zhen Zhang: Conceptualization, Methodology, Writing - original draft, Writing - review & editing, Supervision, Funding acquisition. **Yi Zhang:** Formal analysis, Validation, Writing - original draft. **Liquan Lin:** Formal analysis, Validation, Writing - original draft. **Jinhong Wu:** Formal analysis, Validation. **Haishen Yu:** Investigation. **Xin Pan:** Data curation, Investigation. **Guangliang Li:** Data curation, Investigation. **Jie Wu:** Resources, Supervision. **Tao Xue:** Formal analysis, Software, Validation, Writing - original draft, Funding acquisition.

Declaration of competing interest

The authors declare that they have no known competing financial interests or personal relationships that could have appeared to influence the work reported in this paper.

Acknowledgement

This research is supported by National Natural Science Foundation of China (NSFC) under Grant No. 51705171, Nature Science Foundation of Hubei Province under Grant No. 2019CFB742, Local Innovative and Research Team Project of Guangdong Pearl River Talents Program under Grant No. 2017BT01G167 and Hubei Provincial Training Program of Innovation and Entrepreneurship for Undergraduates (HT2019005).

References

Bains, P.S., Sidhu, S.S., Payal, H.S., 2018a. Investigation of magnetic field-assisted edm of composites. Mater. Manuf. Process. 33, 670–675.
Bains, P.S., Sidhu, S.S., Payal, H.S., 2018b. Magnetic field assisted edm: new horizons for improved surface properties. Siliconindia 10, 1275–1282.
Bhushan, R.K., 2013. Optimization of cutting parameters for minimizing power consumption and maximizing tool life during machining of al alloy sic particle composites. J. Clean. Prod. 39, 242–254.
Chattopadhyay, K.D., Satsangi, P.S., Verma, S., Sharma, P.C., 2008. Analysis of rotary electrical discharge machining characteristics in reversal magnetic field for copper-en8 steel system. Int. J. Adv. Manuf. Technol. 38, 925–937.
Chen, Z., Zhang, Y., Zhang, G., Huang, Y., Liu, C., 2017. Theoretical and experimental study of magnetic-assisted finish cutting ferromagnetic material in wedm. Int. J. Mach. Tool Manufact. 123, 36–47.
Du, J., Ming, W., Cao, Y., He, W., Li, X., 2019. Particle removal mechanism of high volume fraction SiC_p/Al composites by single diamond grit tool. J. Wuhan Univ. Technol.-Materials Sci. Ed. 34, 324–331.
E, PA, U.S., 2012. Report to Congress on Black Carbon, Department of the Interior, Environment, and Related Agencies Appropriations Act 2010. EPA-450/R-12-001.
E, PA, U.S., 2018. Overview of Greenhouse Gases. https://www.epa.gov/ghgemissions/overview-greenhouse-gases.
Gamage, J.R., DeSilva, A.K., Chantzis, D., Antar, M., 2017. Sustainable machining: process energy optimisation of wire electrodischarge machining of inconel and titanium superalloys. J. Clean. Prod. 164, 642–651.
Gamage, J.R., DeSilva, A.K., Harrison, C.S., Harrison, D.K., 2016. Process level environmental performance of electrodischarge machining of aluminium (3003) and steel (aisi p20). J. Clean. Prod. 137, 291–299.
Garg, A., Lam, J.S.L., 2016. Modeling multiple-response environmental and manufacturing characteristics of edm process. J. Clean. Prod. 137, 1588–1601.
Gururaja, S., Ramulu, M., Pedersen, W., 2013. Machining of mmcs: a review. Mach. Sci. Technol. 17, 41–73.
Heinz, K., Kapoor, S., DeVor, R., Surla, V., 2011. An investigation of magnetic-field-assisted material removal in micro-edm for nonmagnetic materials. Journal of Manufacturing Science and Engineering, Transactions of the ASME 133.
Kandpal, B.C., kumar, J., Singh, H., 2015. Machining of aluminium metal matrix composites with electrical discharge machining - a review. Mater. Today: Proceedings 2, 1665–1671, 4th International Conference on Materials Processing and Characterzation.
Kou, Z., Han, F., 2018. On sustainable manufacturing titanium alloy by high-speed edm milling with moving electric arcs while using water-based dielectric. J. Clean. Prod. 189, 78–87.
Leonard, R., Zulfikar, R., Stansbury, R., 2020. Coal mining and lung disease in the 21st century. Curr. Opin. Pulm. Med. 26, 135–141.
Leung, C.C., Yu, I.T.S., Chen, W., 2012. Silicosis. Lancet 379, 2008–2018.
Mahdavinejad, R., Tolouei-Rad, M., Sharifi-Bidgoli, H., 2005. Heat transfer analysis of edm process on silicon carbide. Int. J. Numer. Methods Heat Fluid Flow 15, 483–502.
Maher, I., Sarhan, A.A., Barzani, M.M., Hamdi, M., 2015. Increasing the productivity of the wire-cut electrical discharge machine associated with sustainable production. J. Clean. Prod. 108, 247–255.
Masoudi, M., Gerami, S., 2017. Status of co as an air pollutant and its prediction, using meteorological parameters in esfahan, Iran. Pollution 3, 527–537.
Mathew, J., Sivapirakasam, S., Mahadevan, S., 2010a. Analysis of aerosol emission and hazard evaluation of electrical discharge machining (edm) process. Ind. Health 48, 478–486.
Mathew, J., Sivapirakasam, S., Mahadevan, S., 2010b. Evaluation of occupational exposure to aerosol emitted from die sinking electrical discharge machining process. Int. J. Environ. Health 4.
Ming, W., Jia, H., Zhang, H., Zhang, Z., Liu, K., Du, J., Shen, F., Zhang, G., 2020. A comprehensive review of electric discharge machining of advanced ceramics. Ceram. Int. 46 (14), 21813–21838.
Ming, W., Ma, J., Zhang, Z., Huang, H., Shen, D., Zhang, G., Huang, Y., 2016. Soft computing models and intelligent optimization system in electro-discharge machining of sic/al composites. International Journal of Advanced Manufacturing Technology Soft computing models and intelligent optimization system in electro-discharge machining of SiC/Al composites 87, 201–217.
Ming, W., Zhang, Z., Wang, S., Zhang, Y., Shen, F., Zhang, G., 2019. Comparative study of energy efficiency and environmental impact in magnetic field assisted and conventional electrical discharge machining. J. Clean. Prod. 214, 12–28.
National-Research-Council, 2000. Copper in Drinking Water. The National Academies Press (US, Washington, DC.
Pramanik, A., 2014. Developments in the non-traditional machining of particle reinforced metal matrix composites. Int. J. Mach. Tool Manufact. 86, 44–61.
Saxena, K.K., Agarwal, S., Das, R., 2018. Evaluation of micro-edm (μedm) characteristics of conductive silicon carbide using a coupled thermo-structural process model. J. Adv. Manuf. Syst. 17, 415–443.
Sivapirakasam, S., Mathew, J., Surianarayanan, M., 2011. Constituent analysis of aerosol generated from die sinking electrical discharge machining process. Process Saf. Environ. Protect. 89, 141–150.
Sun, J., Fang, W., Palade, V., Wu, X., Xu, W., 2011. Quantum-behaved particle swarm optimization with Gaussian distributed local attractor point. Appl. Math. Comput. 218, 3763–3775.
Tang, L., Ren, L., Zhu, Q.L., 2018. Edm multi-pulse temperature field simulation of sic/al functionally graded materials. Int. J. Adv. Manuf. Technol. 97, 2501–2508.
USITC, 2009. How the Doc Defines Sustainable Manufacturing. www.trade.gov.
Valaki, J., Rathod, P., 2015. Assessment of Operational Feasibility of Waste Vegetable Oil Based Bio-Dielectric Fluid for Sustainable Electric Discharge Machining

(Edm). The International Journal of Advanced Manufacturing Technology.
Valaki, J., Rathod, P., Khatri, B., 2014. Environmental impact, personnel health and operational safety aspects of electric discharge machining: a review. Proc. IME B J. Eng. Manufact. 229.
Xiong, B., Xu, Z., Yan, Q., Lu, B., Cai, C., 2011. Effects of sic volume fraction and aluminum particulate size on interfacial reactions in sic nanoparticulate reinforced aluminum matrix composites. J. Alloys Compd. 509, 1187–1191.
Zhang, Y., Zhang, Z., Zhang, G., Li, W., 2020a. Reduction of energy consumption and thermal deformation in wedm by magnetic field assisted technology. International Journal of Precision Engineering and Manufacturing-Green Technology 7, 391–404.
Zhang, Z., Huang, H., Ming, W., Xu, Z., Huang, Y., Zhang, G., 2016. Study on machining characteristics of wedm with ultrasonic vibration and magnetic field assisted techniques. J. Mater. Process. Technol. 234, 342–352.
Zhang, Z., Ming, W., Zhang, Y., Yin, L., Xue, T., Yu, H., Chen, Z., Liao, D., Zhang, G., 2020b. Analyzing sustainable performance on high-precision molding process of 3d ultra-thin glass for smart phone. J. Clean. Prod. 255, 120196.
Zhang, Z., Yu, H., Zhang, Y., Yang, K., Li, W., Chen, Z., Zhang, G., 2018. Analysis and optimization of process energy consumption and environmental impact in electrical discharge machining of titanium superalloys. J. Clean. Prod. 198, 833–846.
Zhang, Y., Zhang, Z., Zhang, Y., Liu, D., Wu, J., Huang, Y., Zhang, G., 2020c. Study on machining characteristics of magnetically controlled laser induced plasma micro-machining single-crystal silicon. J. Adv. Res. https://doi.org/10.1016/j.jare.2020.12.005. In press.